

平成 2 4 年 度

京 都 大 学 大 学 院 理 学 研 究 科

D C 3 回 生 研 究 発 表 会
要 旨 集

2 0 1 3 年 1 月 2 1 日 (月)

物 理 学 第 一 分 野

物理学第一分野DC3回生研究発表会

場所：理学研究科5号館 5階・第四講義室
発表：15分（別に質問10分程度）

2013年1月21日（月）9：00～ 開始

目 次

1. Steplike electric conduction in a classical two-dimensional electron system through a narrow constriction in a microchannel
荒木 元 (9 : 0 0) 1
2. Nonequilibrium Dynamics of Deformable Self-Propelled Particles
市野 悠 (9 : 2 5) 2
3. Non-centrosymmetric superconductivity in d -electron compounds
江口 学 (9 : 5 0) 3
4. Visualization of the Spatial Distribution of Order Parameter in Superfluid ^3He with Nuclear Magnetic Resonance Imaging
金本 真知 (1 0 : 1 5) 4

1 0 : 4 0 ~ 1 0 : 5 0 休憩

5. Novel ferromagnetic quantum criticality in the heavy-fermion iron oxypnictide $\text{Ce}(\text{Ru}_{1-x}\text{Fe}_x)\text{PO}$
北川 俊作 (1 0 : 5 0) 5
6. Vacancy trapping and spin-flip transitions of paraexcitons in cuprous oxide studied by visible and terahertz spectroscopy
Sandhaya Koirala (1 1 : 1 5) 6
7. Controlling the Dynamics of a Localized Domain in an Excitable Reaction-Diffusion System by a Time-Delayed Feedback
設楽 恭平 (1 1 : 4 0) 7
8. Nonlinear Transport Phenomena in Semiconductor Studied by Terahertz Nonlinear Spectroscopy
篠北 啓介 (1 2 : 0 5) 8

1 2 : 3 0 ~ 1 3 : 3 0 昼休み

9. An $\text{SU}(6)$ Mott insulator of an atomic Fermi gas realized by large-spin Pomeranchuk cooling
田家慎太郎 (1 3 : 3 0) 9
- 1 0. Mesoscopic Heterogeneity and large response to external fields in Glassy Ferroelectric Crystals
高江 恭平 (1 3 : 5 5) 1 0

1 1. Ultrafast Carrier Dynamics in Graphene under a High Electric Field
谷 峻太郎 (14 : 20) 11

1 2. Resistance Enhancement in the $\nu = 2/3$ Quantum Hall State
津田 是文 (14 : 45) 12

15 : 10 ~ 15 : 20 休憩

1 3. Novel mesophase in the region between Cholesteric and Perforated Lamellar Nematic phases
吉岡 潤 (15 : 20) 13

Steplike electric conduction in a classical two-dimensional electron system through a narrow constriction in a microchannel

Advanced statistical dynamics group Moto Araki

Abstract Using molecular dynamics simulation, we investigate transport properties of a classical two-dimensional electron system confined in a microchannel with a narrow constriction. The calculated conductance in the simulations exhibits steplike increases as reported in a recent experiment [1].

© 2013 Department of Physics, Kyoto University

Using molecular dynamics simulations, we investigate transport properties of classical two-dimensional electrons through a microchannel with a narrow constriction. The electrons are confined by the electric potential derived from the Poisson equation under boundary conditions to imitate a device structure in an experiment, and interact with each other. The electron system of our simulation is a realistic model for strongly correlated electrons on liquid helium in the microscale device. In the simulations, the electrons are driven by the chemical potential difference between two particle baths.[2]

As a function of the confinement strength of the constriction, the calculated conductance in the simulations exhibits steplike increases as reported in a recent experiment [1]. It is confirmed that the number of the steps corresponds to the number of stream lines of electrons through the constriction. For the strong confinement, the conductance is affected by the temporal fluctuation of electrostatic potential which induces intermittent disappearances of a potential barrier in the constriction. We also observe the temporal change of the number of electrons' streams through the constriction because of the short-wavelength density fluctuations [2]. Therefore, we suppose that the stream lines forced by the confinement cause the steplike electric conduction, and the fluctuation plays a certain role in smoothing the steps.

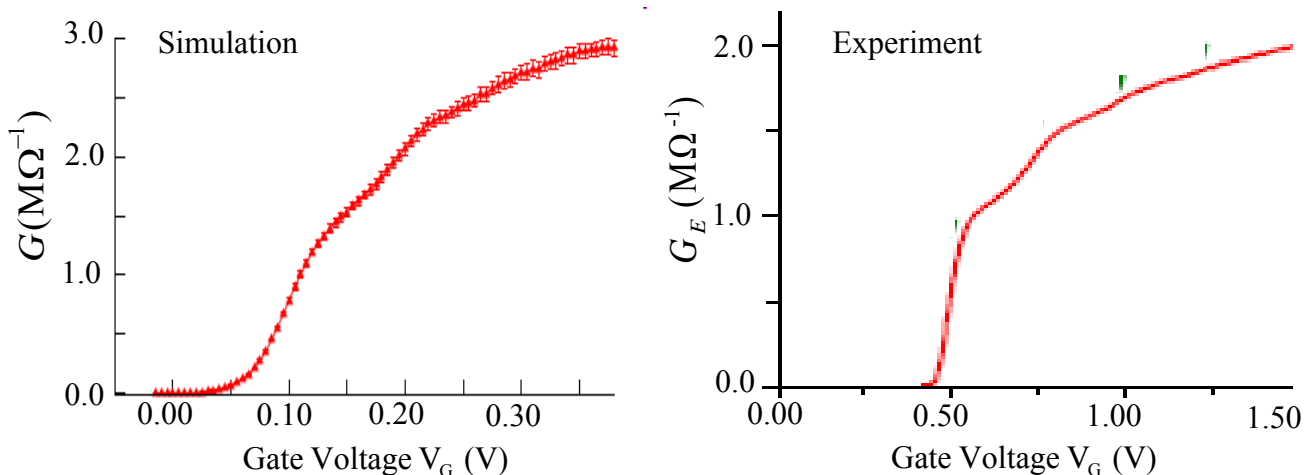


Fig. 1. The calculated conductance G in the simulations (left figure) and the measured conductance G_E in the experiment [1] (right figure) versus the gate voltage V_G . As V_G is lower, the confinement of the constriction is stronger.

References

- [1] D. G. Rees *et al.*, Phys. Rev. Lett. **106**, 026803 (2011).
- [2] M. Araki and H. Hayakawa, Phys. Rev. B **86**, 165412 (2012).

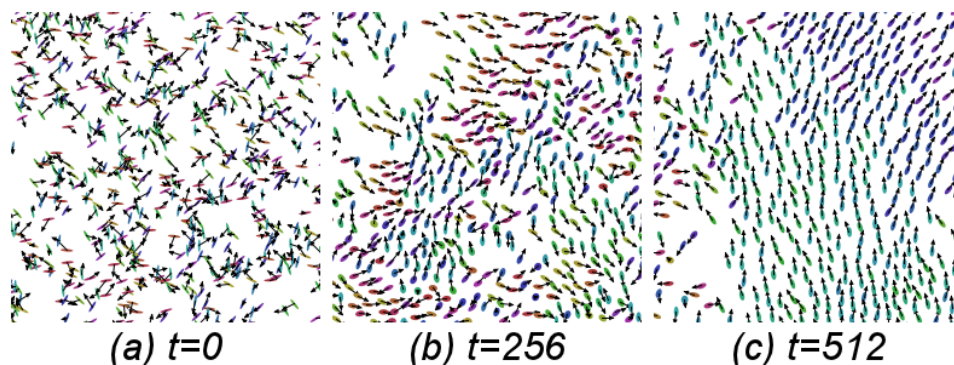
Nonequilibrium Dynamics of Deformable Self-Propelled Particles

Nonlinear Dynamics Group Yu Itino

Abstract We present a theoretical study on assemblies of deformable self-propelled particles (SPP). Starting from the single particle model of a deformable SPP (Ohta-Ohkuma model), we introduced the short-ranged repulsive force between those particles. The system exhibits ordered, disordered, and coexistence state by changing the density and the noise strength. © 2013 Department of Physics, Kyoto University

The spontaneous order of the self-propelled particles (SPP) has been studied over a decade. So called “Vicsek model” [1] and its variants exhibit collective polar order due to the explicit alignment rule between particles. The breakdown of the collective motion under strong external noise has been a main concern of current studies.

In addition to minimal variables of SPP (position and velocity), our deformable SPP has a nematic deformation tensor coupled with the polar velocity [2]. We introduced the short-ranged repulsive interaction between particles, and instead of explicit alignment rule, the deformation-dependent magnitude was included to the multi-particle model [3, 4]. The following figure shows the emergence of the collective (ordered) motion starting from (a) random initial state, followed by (b) intermediate ordered region, and (c) globally ordered structure.



The (polar) order of the system can be destroyed by external randomness. We studied the order-disorder transition induced by increasing density and the noise. The transition is confirmed to be discontinuous, and the hysteresis has been observed. The nature of the transition is qualitatively explained by the mean field theory.

Compared to the diffusive disordered state, the ordered state contains much complex and defective structure. The collective swirling motion within the ordered region has been observed. Furthermore, a novel band structure within the disordered domain, invading ordered region, has been found [5]. To quantitatively address those phenomena, we developed a real-space clustering method to classify ordered domains.

References

- [1] T. Vicsek, *et. al.*, Phys. Rev. Lett. **75** 1226 (1995).
- [2] T. Ohta and T. Ohkuma: Phys. Rev. Lett. **102** 154101 (2009).
- [3] Y. Itino, T. Ohkuma, and T. Ohta, J. Phys. Soc. Jpn. **80** 033001 (2011).
- [4] Y. Itino, and T. Ohta, J. Phys. Soc. Jpn. **81** 104007 (2012).
- [5] M. Tarama, Y. Itino, A. M. Menzel, and T. Ohta, EPJ (to be published).

Non-centrosymmetric superconductivity in *d*-electron compounds

Quantum Materials Laboratory Gaku EGUCHI

Abstract Superconductivity in the absence of crystalline inversion symmetry in *d*-electron compounds is studied. We succeeded in growing polycrystalline CaMSi_3 ($M=\text{Ir, Pt}$) and single-crystalline CaIrSi_3 , and revealed their superconducting behavior. We also studied the novel spin singlet-triplet mixed superconducting state in $\text{Li}_2(\text{Pd}_{1-x}\text{Pt}_x)_3\text{B}$.

© 2013 Department of Physics, Kyoto University

Superconductivity in the absence of inversion symmetry has been attracting much attention because of its potential exotic superconducting phenomena. In bulk materials, such superconductivity is realized in crystals without inversion centers; these superconductors are nowadays called the non-centrosymmetric superconductors[1]. The absence of inversion symmetry results in two important features. First, the superconducting state can no longer be classified either as a spin-singlet or a spin-triplet state, but is a singlet-triplet mixed state. Second, the electronic energy bands exhibit a momentum-dependent effective Zeeman splitting due to the antisymmetric spin-orbit interaction.

We studied some *d*-electron-based non-magnetic non-centrosymmetric superconductors. These compounds should be appropriate to examine the novel pairing state because novel features specific to non-centrosymmetric superconductivity can be extracted without other physics such as strong electron correlations and magnetism.

We succeeded in growing polycrystalline CaMSi_3 ($M=\text{Ir, Pt}$) (Fig. 1, left) and revealed their fully-gapped superconducting nature and the dominance of electron-phonon scattering[2,3]. What is more, we also succeeded in growing single-crystalline CaIrSi_3 and revealed the presence of strong spin-orbit interaction and weakly anisotropic superconducting nature[4]. We also investigated physical properties of polycrystalline $\text{Li}_2(\text{Pd}_{1-x}\text{Pt}_x)_3\text{B}$ (Fig.1, right) systematically, and revealed a phonon anomaly as well as anisotropic superconducting gaps in Pt-rich members, including their magnetic field dependence[5].

Among these works done in my Ph. D course, I focus on the single-crystalline CaIrSi_3 for this presentation. I explain single-crystal growth of CaIrSi_3 and its normal and superconducting properties, and then discuss the possibility of a novel spin singlet-triplet mixed state.

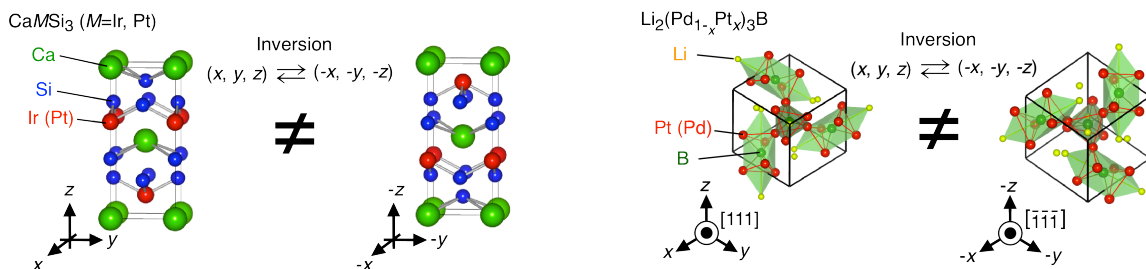


Fig. 1. Crystal structures and their inversion of non-centrosymmetric CaMSi_3 ($M=\text{Ir, Pt}$) and $\text{Li}_2(\text{Pd}_{1-x}\text{Pt}_x)_3\text{B}$. The figures are drawn by VESTA[6].

References

- [1] E. Bauer *et al.*, Phys. Rev. Lett. **92**, 027003 (2004).
- [2] G. Eguchi *et al.*, Phys. Rev. B **83**, 024512 (2011).
- [3] G. Eguchi *et al.*, J. Phys. Soc. Jpn. **81**, 074711 (2012).
- [4] G. Eguchi *et al.*, Phys. Rev. B **86**, 184510 (2012).
- [5] D. C. Peets, G. Eguchi *et al.*, Phys. Rev. B **81**, 054521 (2011), etc.
- [6] K. Momma and F. Izumi, J. Appl. Crystallogr. **44**, 1272 (2011).

Visualization of the Spatial Distribution of Order Parameter in Superfluid ^3He with Nuclear Magnetic Resonance Imaging

Low Temperature Physics Laboratory Masatomo Kanemoto

Abstract Resonance frequency of superfluid ^3He in NMR depends on the local orientation of internal degree of freedom of the order parameter. I developed the method for visualizing the spatial distribution of resonance frequency in NMR in order to study inhomogeneous order parameter in superfluid ^3He .

© 2013 Department of Physics, Kyoto University

Superfluid ^3He is a p-wave pair condensate with multiple internal degrees of freedom. So superfluid ^3He has some phases. In the A-phase, the order parameter is expressed by two vectors, \mathbf{d} and \mathbf{l} . The spatial distribution of the order parameter is called as the texture. The texture is determined by minimizing the total energy, which depends on applied magnetic fields and the shape of the container wall. NMR signals in A-phase are characterized by a frequency shift from Larmor frequency which is determined by applied magnetic field. The frequency shift depends on the distribution of the order parameter. In standard NMR, the signal is integrated over the space in the container. No information on the location of signal source can be obtained. NMR spectrum under various magnetic field gradient direction provide MRI image, which is a spatial distribution of signal source. However in the standard MRI, spectroscopic information is destroyed. In order to measure the distribution of the frequency shift in space, I developed frequency-resolved MRI method.

A parallel plate cell whose gap is 100 microns is constructed. Static magnetic field is applied parallel to the plate. In A-phase, \mathbf{l} orients perpendicular to the wall of the container, while \mathbf{d} tends to be perpendicular to the magnetic field. The \mathbf{d} and \mathbf{l} orients parallel or anti-parallel with each other due to dipole interaction. A homogeneous texture, in which \mathbf{d} and \mathbf{l} are perpendicular to the plates, satisfies all these conditions. If there are parallel and anti-parallel domains, where \mathbf{d} and \mathbf{l} orient parallel or anti-parallel with each other, there appears a region where \mathbf{d} and/or \mathbf{l} rotate gradually in space in order to connect domains on each side. This region is called the domain wall. Such a domain wall was observed by NMR measurement previously. However nobody has ever studied why this energetically unfavorable state can be stabilized. The MRI measurement of the topological objects in superfluid ^3He , such as the domain wall, opens the doorway to further understand topological superfluid.

To demonstrate the frequency-resolved MRI, spatial variation of the static magnetic field strength in the parallel plate cell is measured (Fig.1). The bright circle corresponds to the sensitive region of the NMR coil in the plate. Gradations inside the circle indicate the strength of local magnetic field in 57Hz step at the Larmor frequency of 5.4MHz. The NMR spectrum shows the corresponding lineshape with long tail on low frequency side (Fig.2). Saddle shaped distribution of the static magnetic field in Fig.1 explains the lineshape in Fig.2 very well. This indicates the feasibility of the frequency-resolved MRI as advanced NMR spectroscopic measurement.

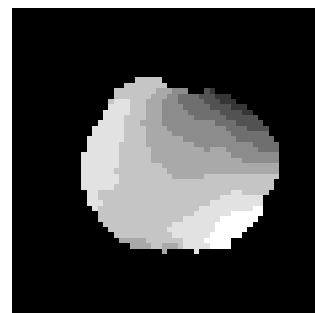


Fig. 1

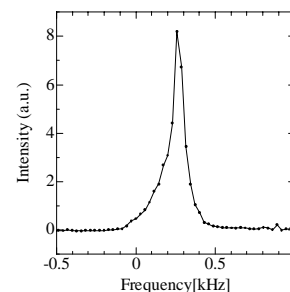


Fig. 2

Novel ferromagnetic quantum criticality in the heavy-fermion iron oxypnictide $\text{Ce}(\text{Ru}_{1-x}\text{Fe}_x)\text{PO}$

Quantum Materials Lab. Shunsaku Kitagawa

Abstract We have performed ^{31}P -NMR measurements on $\text{Ce}(\text{Ru}_{1-x}\text{Fe}_x)\text{PO}$ in order to investigate ferromagnetic (FM) quantum criticality. Our NMR results suggest that the FM quantum critical point at $x \sim 0.86$ is induced by the tuning of the magnetic dimensionality, different mechanism from that believed in heavy-fermion compounds.

© 2013 Department of Physics, Kyoto University

Quantum phase transition in itinerant magnets is one of the major topics in a strongly correlated electron system. Up to now, there have been considerable efforts for understanding the nature of a QCP on various antiferromagnetic heavy fermion (HF) compounds, but very few on ferromagnetic (FM) HF compounds, particularly on Ce-based FM HF compounds. The iron oxypnictide $\text{CeFe}(\text{Ru})\text{PO}$ is a related material of the iron-based superconductor LaFePO . They possess the same 2D layered structure, stacking the Ce(La)O and Fe(Ru)P layers alternatively. The CeO layer contributes to the large magnetic response, and the Fe(Ru)P layer is conductive in $\text{CeFe}(\text{Ru})\text{PO}$. CeRuPO is a FM HF system with Curie temperature $T_{\text{Curie}} = 15$ K and coherent temperature $T_K \sim 10$ K[1]. On the other hand, counterpart CeFePO is a HF compound with a PM ground state down to 80 mK and $T_K \sim 10$ K[2,3]. Therefore, we expect that the ground state can be tuned continuously from FM to PM state by substituting isovalent Fe for Ru.

We performed ^{31}P -NMR on $\text{Ce}(\text{Ru}_{1-x}\text{Fe}_x)\text{PO}$ to investigate the evolution of magnetic properties at low temperatures. NMR measurements can probe static and dynamic magnetic properties. Knight shift K detects static spin susceptibility at $q = 0$, while nuclear spin-lattice relaxation rate $1/T_1$ probes q -summed spin fluctuations perpendicular to the applied magnetic field. T_{Curie} and the internal field at the P site, proportional to ordered magnetic moment $\langle \mu_{\text{ord}} \rangle$, continuously approach zero toward $x \sim 0.86$ by Fe substitution for Ru, suggestive of the presence of FM QCP at $x \sim 0.86$ (Figure) [4], which is in sharp contrast with FM criticality observed in other FM compounds. For example, FM transition in UGe_2 is gradually suppressed by applying pressure, but the transition changes from second order to first order at a tricritical point and the first order metamagnetic transition emerges in a small external field[5].

In addition, we discussed the variation of magnetic-fluctuation character in $\text{Ce}(\text{Ru}_{1-x}\text{Fe}_x)\text{PO}$ from the relationship between K and $1/T_1$. Our experimental results suggest that the FM QCP in $\text{Ce}(\text{Ru}_{1-x}\text{Fe}_x)\text{PO}$ is induced by the tuning of the dimensionality of the magnetic correlations from three dimensionality to two dimensionality. This mechanism is quite different from that believed in HF compounds and itinerant FM compounds, rather similar to the dimensional tuning realized in superlattice $\text{CeIn}_3/\text{LaIn}_3$ [6]. The phase diagram difference between $\text{Ce}(\text{Ru}_{1-x}\text{Fe}_x)\text{PO}$ and the other FM systems may originate from the difference of the tuning parameter.

References

- [1] C. Krellner *et al.*, Phys. Rev. B **76**, 104418 (2007).
- [2] E. Brüning. *et al.* Phys. Rev. Lett. **101**, 117206 (2008).
- [3] S. Kitagawa *et al.*, Phys. Rev. Lett. **107**, 277002 (2011).
- [4] S. Kitagawa *et al.*, Phys. Rev. Lett. **109**, 227004 (2012).
- [5] H. Kotegawa *et al.*, J. Phys. Soc. Jpn. **80**, 083703 (2011).
- [6] H. Shishido *et al.*, Science **327**, 980-983 (2010).

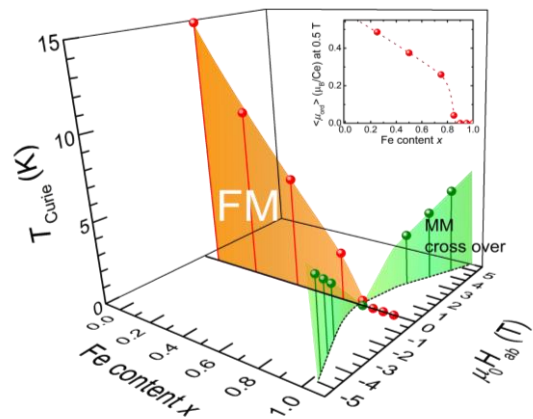


Figure: The T - x - H phase diagram on $\text{Ce}(\text{Ru}_{1-x}\text{Fe}_x)\text{PO}$ obtained by ^{31}P -NMR. The inset shows x dependence of ordered magnetic moment $\langle \mu_{\text{ord}} \rangle$ at $\mu_0 H \approx 0.5$ T.

Vacancy trapping and spin-flip transitions of paraexcitons in cuprous oxide studied by visible and terahertz spectroscopy

Solid State Spectroscopy Group

Sandhaya Koirala

Abstract We have investigated the trapping mechanism of free excitons into crystal defects in a semiconductor cuprous oxide. By using high grade samples containing small amounts of oxygen vacancies, we find the direct correlation between the lifetimes of free paraexcitons and trapped paraexcitons. In addition, we have designed terahertz time-domain spectroscopic measurements for the detection of paraexcitons.

© 2013 Department of Physics, Kyoto University

An ensemble of excitons or bound electron-hole pairs in a semiconductor is predicted to undergo a transition into a Bose-Einstein condensation (BEC) phase at low temperatures. Due to the long lifetime, 1s paraexcitons in cuprous oxide (Cu_2O) are believed to be a good candidate to realize excitonic BEC in a thermal equilibrium [1]. To investigate excitonic BEC states, two parameters are very important; one is the exciton lifetime and the other is the exciton density. Since the lifetime of the 1s paraexcitons in Cu_2O is limited by some unknown non-radiative recombination processes, we clarified the lifetime shortening mechanism by visible spectroscopy. In addition, we propose a novel technique of monitoring the paraexciton density by using spin-flip transitions in the terahertz region.

We performed time-resolved spectroscopic measurements by taking natural crystals of cuprous oxide containing various amounts of oxygen vacancy. Based on the temperature dependence of the photoluminescence spectra, we obtained the activation energy of $E_A=33$ meV for trapping of free excitons into oxygen vacancy. We found the correlation between lifetimes of free and trapped excitons (Fig.1a), and established four-level energy model to explain the temperature dependent lifetimes (Fig.1b). From the comparative studies of four different samples, it is clear that the existence of the oxygen vacancy is crucial in limiting the free-exciton lifetime in high-quality cuprous oxide [2].

So far, excitonic Lyman spectroscopy has been performed to determine the 1s paraexciton density [3]. This method induces a transition from 1s to 2p paraexcitons separated by 129 meV, accompanying emission of many phonons and possible unwanted heating. Here, we propose to use the recent terahertz technology to monitor the spin-flip transition of 1s paraexcitons, from the triplet to the singlet states separated by 12 meV. We calculated selection rules for these spin-flip transitions under external magnetic fields. Using a strong terahertz generation system which we recently build and checked the performance, we will perform optical-pump and terahertz-probe experiments. Our method is expected to be useful in detecting an excitonic BEC state in a potential well created by stress under a strong magnetic field at low temperatures [4].

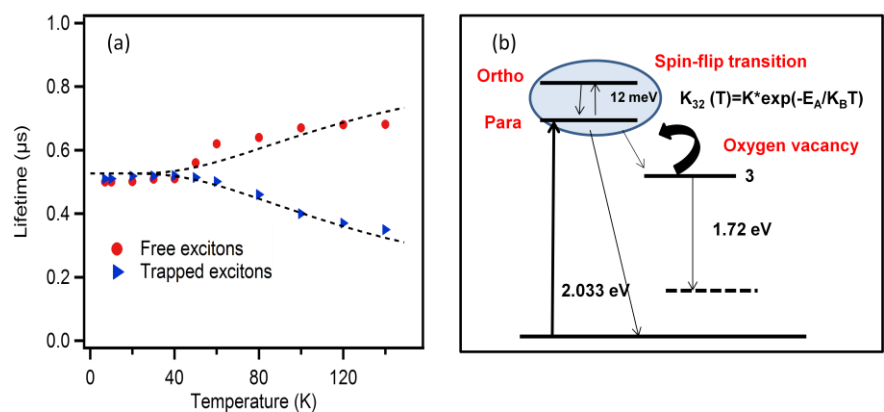


Figure 1: (a) Lifetimes of free and trapped excitons as a function of temperature. Simulated lifetimes are shown by dashed lines. (b) Schematic diagram of the four-level scheme used for the simulation.

Reference:

- [1] K. Yoshioka et al., Nature Commun. **2** (2011) 328.
- [2] S. Koirala et al., Journal of Lumin **134** (2013) 524.
- [3] T. Tayagaki et al., J. Phys. Soc. Jpn. **74** (2005) 1423.
- [4] Ch. Standford et al., Phys. Rev. B **84** (2011) 165215.

Controlling the Dynamics of a Localized Domain in an Excitable Reaction-Diffusion System by a Time-Delayed Feedback

Nonlinear Dynamics Group Kyohei Shitara

Abstract We introduce a time-delayed feedback to reaction-diffusion equations having a solution of a localized domain. As the result of it, it is found that we can make a motionless domain traveling and a traveling domain motionless by changing a sign of the feedback strength. In addition to it, a variety of other behaviors are also found.

© 2013 Department of Physics, Kyoto University

A reaction-diffusion system is one of dissipative systems and exhibits a variety of pattern formation phenomena. To reveal the dynamics of these patterns has great potential for applications as well as contributions to an investigation of non-equilibrium systems. Many scientists try to control the dynamics of these patterns.

A localized domain is one of patterns in reaction-diffusion systems. It is known that there is a drift bifurcation where a motionless domain becomes unstable and begins to travel [1, 2]. However, whether its bifurcation can be realized or not in experiments depends on systems. Therefore, we have tried to control a motion of a localized domain.

Tlidi and his co-workers have shown that a motionless cavity soliton can be driven by a time-delayed feedback [3]. Following their method, we have introduced a time-delayed feedback to reaction-diffusion equations having excitability in one dimension as shown below.

$$\tau\varepsilon\frac{\partial u}{\partial t} = \varepsilon^2\frac{\partial^2 u}{\partial x^2} + f(u) - v + \Lambda[u(t-T) - u(t)]$$

$$\frac{\partial v}{\partial t} = D\frac{\partial^2 v}{\partial x^2} + u - \nu$$

where Λ and T are the strength of the delayed feedback and the delay time, respectively. We have found that when the sign of Λ is negative, a motionless domain becomes unstable and begins to travel as shown in Fig. 1(a). On the other hand, when the sign of Λ is positive, a traveling domain becomes unstable and motionless as shown in Fig. 1(b). Moreover, a variety of other behaviors of the domain are also found such as traveling with oscillation, rocking, and creation-annihilation.

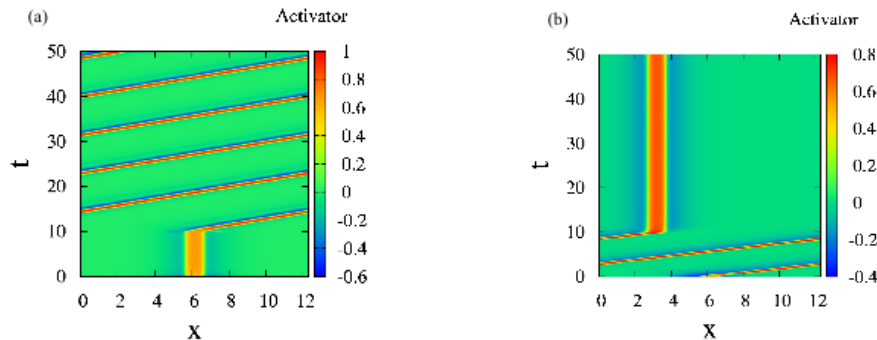


Fig. 1. (a) A motionless domain begin to travel at $t=10$ when Λ is negative. (b) A traveling domain become motionless at $t=10$ when Λ is positive.

References

- [1] T. Ohta, Physica D, **151**, 61 (2001).
- [2] K. Krischer, A. Mikhailov, Phys. Rev. Lett. **73**, 3165 (1994).
- [3] M. Tlidi, A. G. Vladimirov, D. Pieroux, and D. Turaev, Phys. Rev. Lett. **103**, 103904 (2009)

Nonlinear Transport Phenomena in Semiconductor Studied by Terahertz Nonlinear Spectroscopy

Solid State Spectroscopy Group

Keisuke Shinokita

Abstract I will present that the intense THz pulses induce strong spectral modulations in excitonic and band-edge absorption of GaAs/AlGaAs multiple quantum wells. Furthermore, it is introduced that the 1-MV/cm electric field of a THz pulse allows us to excite electrons from valence to conduction band of GaAs/AlGaAs MQW and observe bright exciton luminescence.

© 2013 Department of Physics, Kyoto University

The nonlinear interaction of matter with strong, oscillating electric fields has attracted considerable attention because of their importance in fundamental physics and technological applications. The resonant (or nearly resonant) interaction of electric fields with electronic transitions in semiconductors and atomic gases exhibits intriguing nonlinear phenomena such as the ac (optical) Stark effect, Rabi oscillations, Autler-Townes splitting, and electromagnetically induced transparency. Even in nonresonant situations, atomic and condensed matter systems subjected to high-intensity laser excitation exhibit extreme nonlinear phenomena such as above-threshold ionization, high-order harmonic generation and various nonlinear transport phenomena. These phenomena cannot be described by perturbation theory. The recent developments in high-power table-top terahertz (THz) pulse sources enable us to coherently drive low-energy transitions into the nonlinear regime and to study fascinating nonlinear transport phenomena in various materials [1].

In this work we studied the nonlinear interaction of excitons and bandgap in GaAs/AlGaAs multiple quantum wells (QWs) by using THz-pump (below 0.1 MV/cm) and optical-probe spectroscopy [2]. This technique revealed that the intense single-cycle THz pulses induce strong spectral modulations in the excitonic and band-edge absorption of QWs. Furthermore, by using the ultra-intense THz pulse (a 1 MV/cm electric field it is indicated that it allows us to excite electrons from the valence band to the conduction band of the QWs and observe exciton luminescence [3]. To obtain the influences of trap states on the nonlinear transport phenomena under instantaneous high-electric fields, we studied the photoexcited carrier dynamics in cleaner QWs by using time-resolved photoluminescence spectroscopy involving the simultaneous use of continuous-wave visible laser and intense THz pulse excitations [4]. It is found that the intense THz pulse induces the photoluminescence (PL) flash from the undoped QWs under continuous wave laser excitation, and the number of excitons increases by four orders of magnitude compared with the steady-state exciton density. Furthermore, the absence of THz-induced exciton generation in this study suggests that in high-quality GaAs wells, the preservation of the k-conservation rule because of lack of impurity or defect states significantly suppresses the impact ionization rate.

References

- [1] H. Hirori, A. Doi, F. Blanchard, and K. Tanaka, *Appl. Phys. Lett.* **98**, 091106 (2011).
- [2] K. Shinokita, H. Hirori, M. Nagai, N. Satoh, Y. Kadoya, and K. Tanaka, *Appl. Phys. Lett.* **97**, 211902 (2010).
- [3] H. Hirori, K. Shinokita, M. Shirai, S. Tani, Y. Kadoya, and K. Tanaka, *Nature Commun.* **2**, 594 (2011).
- [4] K. Shinokita, H. Hirori, K. Tanaka, T. Mochizuki, C. Kim, H. Akiyama, L. N. Pfeiffer, and K. W. West, submitted for publication.

An SU(6) Mott insulator of an atomic Fermi gas realized by large-spin Pomeranchuk cooling

Quantum Optics Group Shintaro Taie

Abstract We report the realization of a Mott insulator of an atomic Fermi gas with novel SU(6) spin symmetry. Besides several characteristics of a Mott phase such as vanishing compressibility, we find the strong adiabatic cooling effect which originates from its large spin degree of freedom.

© 2013 Department of Physics, Kyoto University

The SU(N) Hubbard model, which is obtained by extending SU(2) spin symmetry of the usual Hubbard model to SU($N > 2$), has attracted much theoretical interests in the context of searching for the ground states without long-range order, such as spin liquids [1].

We report the first experimental realization of a Mott insulator with enlarged SU(N) spin symmetry, with an atomic Fermi gas of ^{173}Yb in a three-dimensional optical lattice [2]. ^{173}Yb has an SU(6) symmetric interaction with respect to its nuclear spin $I=5/2$ and realizes the SU(6) Hubbard model in the optical lattice. First, we observe several features that is common to Mott insulating phases. By using photoassociation technique, we measure double occupancy in the lattice, and observe the significant reduction of double occupancy in the strongly interacting regime. From this behavior of double occupancy, we extract the compressibility of the system and find it consistent with the emergence of a Mott insulating core with unit filling in the trap center. We also confirm the existence of the charge excitation gap on the order of on-site interaction U , by applying periodic amplitude modulation of the lattice potential.

Lattice modulation spectroscopy can also provide information of nearest-neighbor correlations of atoms in optical lattices [3]. We apply thermometry based on this correlation measurement to both SU(6) and SU(2) systems under the same experimental conditions, and find that the SU(6) system has much lower temperature compared with the SU(2) system (Fig.1). This remarkable result can be attributed to the enhancement of adiabatic cooling during the loading process into the lattice, owing to the large spin degree of freedom in the localized Mott phase. This mechanism is analogous to Pomeranchuk cooling in solid ^3He and advantageous for realizing exotic quantum phases of the SU(N) Hubbard model at extremely low temperature.

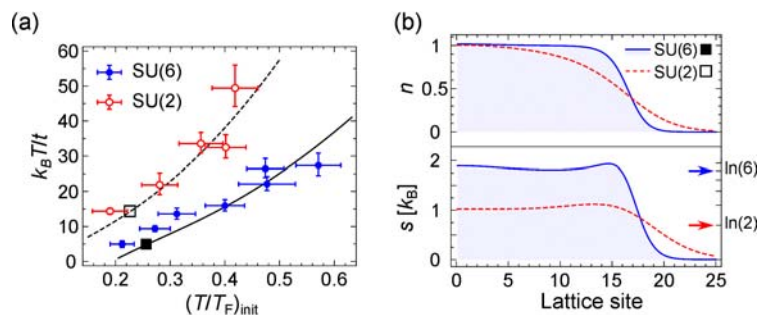


Fig. 1. (a) Measured temperatures of SU(6) (closed circles) and SU(2) (open circles) Mott insulators of ^{173}Yb in a 3D optical lattice. (b) Expected density and entropy profiles for the data with lowest temperatures in (a).

References

- [1] For example, N. Read and S. Sachdev, Nucl. Phys. B 316, 609-640 (1989)
- [2] S. Taie, R. Yamazaki, S. Sugawa and Y. Takahashi, Nature Phys. **8**, 825-830 (2012).
- [3] D. Greif, L. Tarruell, T. Uehlinger, R. Jördens and T. Esslinger, Phys. Rev. Lett. 106, 145302 (2011)

Mesoscopic Heterogeneity and large response to external fields in Glassy Ferroelectric Crystals

Phase Transition Dynamics Group Kyohei Takae

Abstract We construct a molecular dynamics model of glassy ferroelectric crystals, which consist of spheroids possessing dipolar moments and non-polar isotropic impurities. Mesoscopically ordered domains are conspicuous. Large dielectric and piezoelectric responses with hysteresis loops are also marked under applied electric fields at low temperatures.

© 2013 Department of Physics, Kyoto University

Certain crystals composed of anisotropic particles undergo orientation phase transitions at low temperature with spontaneous lattice deformations. With addition of impurities, however, the macroscopic order does not grow at low temperatures, yielding glassy crystalline states [1,2]. In real substances including ferroelectric relaxors, furthermore, molecules often possess dipolar moments, resulting in complex dielectric interactions. For example, nanoscale freezing of ferroelectric domain (polar nanoregions) without ferroelectric phase transitions, and large dielectric constants with characteristic frequency dependence, have been reported [3]. Large piezoelectric responses are also conspicuous in some relaxors [4].

We here present molecular dynamics results of dipolar glass formation in crystals composed of polar spheroids and non-polar isotropic impurities. In these glasses without macroscopic order, heterogeneous distribution of mesoscopically ordered domains are conspicuous, as displayed in the left panel of Fig.1. Under applied electric fields, the glasses exhibit large polarisation responses with hysteresis loops at low temperatures, whereas paraelectric response is observed at high temperatures. This characteristic behaviour of the dipole glasses is displayed in the middle panel and is analogous to ferroelectric materials. Furthermore, since the shape of dipolar particles are anisotropic in our model, changes of the direction of dipolar moments lead to large piezoelectric strain in the glassy ferroelectric crystals, as shown in the right panel of Fig.1.

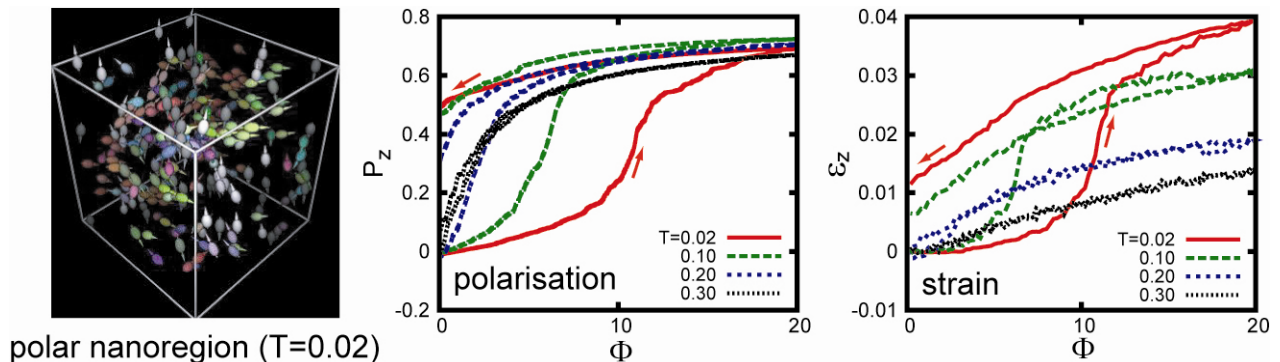


Fig.1. Orientationally ordered domains in a glassy ferroelectric crystal at low temperature T (left). Polarisation and strain response to applied electric field (middle and right). Φ represents the applied voltage.

References

- [1] U. T. Höchli, K. Knorr, and A. Loidl, *Adv. Phys.* **39**, 405-615 (1990).
- [2] K. Takae and A. Onuki, *EPL* **100**, 16006 (2012).
- [3] L. E. Cross, *Ferroelectrics* **76**, 241-267 (1987).
- [4] S.-E. Park and T. R. Shtrout, *J. Appl. Phys.* **82**, 1804-1811 (1997).

Ultrafast Carrier Dynamics in Graphene under a High Electric Field

Solid state spectroscopy group Shuntaro Tani

Abstract Time-resolved high-field carrier transport in graphene is studied using terahertz-pump optical-probe technique. The experimental results show good agreement with our numerical results, which demonstrate the importance of efficient carrier multiplication by impact ionization.

© 2013 Department of Physics, Kyoto University

Graphene is a mono-atomic layer carbon material which possesses many unique properties arising from its truly 2D honeycomb structure. Especially, its characteristic linear dispersion band structure makes electrons massless, which obey the relativistic Dirac equation. Since an electron has a charge, the combination of light and graphene provides us an ideal playground for the relativistic massless particles in solid state, where we can create and manipulate the Dirac fermions, and monitor their dynamics using optical and terahertz (THz) techniques. One major challenge is to understand the electron dynamics under a high electric field, which would establish the foundation of the Dirac fermion transport with many body interaction. Since the momentum distribution of electrons is far out of equilibrium, many body interaction and various scattering processes play dominant roles. This requires ultrafast time resolution for the measurement.

We have investigated the ultrafast carrier dynamics in graphene under high electric fields using 200 fs half-cycle THz excitation pulses and monitoring their dynamics with 50 fs duration near-infrared (NIR) probe pulses [1]. Right after the THz excitation, the transmission of graphene increases and returns back to its initial value within 2 ps. This THz induced transparency is observed for the first time in the NIR region, and should be caused by the electron filling or hole depletion of the corresponding energy levels, allowing us to monitor the time-resolved carrier dynamics under the THz field. Measurements with various THz field strength and quantitative analysis show that the carrier acceleration by the intense THz field is far more efficient than that is expected from the previous models.

To account for our experimental results, we have calculated the distribution function of carriers in the momentum space using the semiclassical Boltzmann equation. What is new in our calculation is that we have included many body interband scattering processes, which changes the number of carriers (i.e., impact ionization and Auger recombination). Although the occurrence of these processes has been controversial, the good agreement between experimental and numerical results demonstrate the importance of efficient carrier multiplication by the impact ionization in graphene.

Figures 1(a)–(e) show calculated distribution of holes in the momentum space at various time delays for the maximum applied electric field of 300 kV/cm. Figures 1(f)–(j) show the corresponding angle-resolved energy distribution of holes. Before THz pulse excitation, holes are distributed within Fermi energy with 300 K thermal fluctuation [Figs. 1(a) and 1(f)]. As a THz electric field is applied, the carrier distribution becomes an asymmetric shape [Figs. 1(b) and 1(g)], and keeps its asymmetry until the peak electric field [Figs. 1(c) and 1(h)]. After the THz excitation pulse is passing through the sample, the distribution immediately recovers its symmetric shape [Figs. 1(d) and 1(i)] and returns back to the initial distribution by emitting optical phonons [Figs. 1(e) and 1(j)].

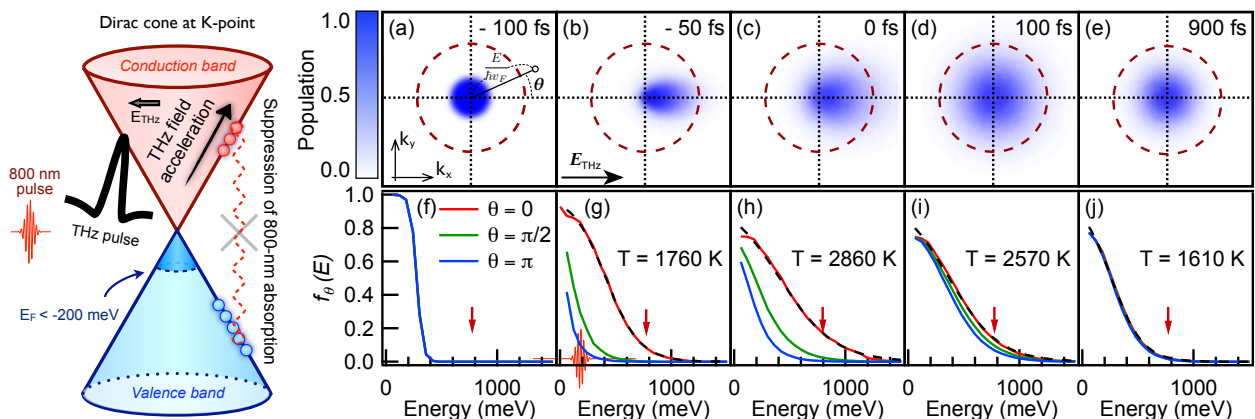


Fig. 1(a)–(e) Distribution function of holes in the momentum space with various time delays. Dashed circles represent momenta corresponding to the energy of 800 nm transition. (f)–(j) Angle-resolved energy distribution of holes. Fermi-Dirac fitting is represented as a dashed line. Vertical arrows indicate the energy of 800 nm transition.

[1] S.Tani, F.Blanchard, and K.Tanaka, Phys. Rev. Lett. **109**, 166603 (2012)

Resistance Enhancement in the $\nu = 2/3$ Quantum Hall State

Nano-scale Quantum Condensed Matter Physics Laboratory Shibun Tsuda

Abstract We have investigated the quantum Hall state where longitudinal resistance R_{xx} is enhanced with nuclear spin polarization induced by large current at the Landau level filling factor $\nu = 2/3$. With the measurement of temperature dependence and pump current frequency dependence of R_{xx} , we find out that the resistance enhanced state is an insulator and is effectively enhanced by AC current.

The spin degree of freedom plays an important role in the fractional quantum Hall States (QHSs). It is responsible for a variety of phenomena such as phase transitions between different ground states and interactions of the electronic system with the nuclei. At the spin phase transition point in $\nu = 2/3$ QHS, an anomalous longitudinal resistance R_{xx} peak is observed. The enhancement of the R_{xx} is explained by a domain structure of the two different spin phases of $\nu = 2/3$ QHS [1]. It is believed that when current pass across a domain boundary, electron spins flip-flop scatter nuclear spins causing dynamic nuclear spin polarization (DNP), then the spin polarization affects back the domain formation and increases the length of the domain boundaries. The nuclear spin relaxation after DNP in the $\nu = 2/3$ QHS is applied to study of various QHSs [2]. However, details of the domain structure and the mechanism of the R_{xx} enhancement are still unclear. Previous experiment couldn't sufficiently study the resistance enhanced state (RES) because the RES is not stable and decays over roughly several hundred seconds.

In our study, we measured the R_{xx} much faster than the decay time. We changed the current to a sufficiently small value 5 nA and measured the temperature dependence of RES within 50 s after DNP at a large current of 60 nA for 2,000 s. Figure 1 shows the temperature T dependence of R_{xx} of after DNP by AC and DC current and before DNP. Surprisingly, we observed an unexpected phenomenon that the derivative of R_{xx} with respect to T is negative after AC current pumping [3]. This result indicates that the enhanced resistance state is an insulating phase transitioned from the QHS. Then, we measured the pump current frequency f_{pump} dependence of RES. Inset of Fig. 2 shows the time evolutions of R_{xx} with several f_{pump} . In Fig. 2, f_{pump} dependence of R_{xx} after 3,600 s pumping are illustrated. Obviously the resistance enhancement effect is large in high f_{pump} and weaken with decreasing f_{pump} . DC pumping causes the small resistance state (~ 5 k Ω) which has positive derivative of R_{xx} with respect to T (Fig. 1). This result suggests that the oscillation of the electric field is an important role for the R_{xx} enhancement.

In this study, we first found that the RES is an insulating phase transitioned from the QHS by AC current. This new discoveries shed new light on the nuclear polarization mechanism in the $\nu = 2/3$ QHS.

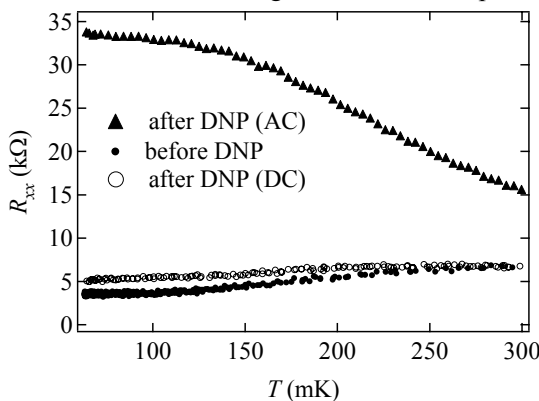


Fig.1. The temperature dependence of R_{xx} after DNP and before DNP.

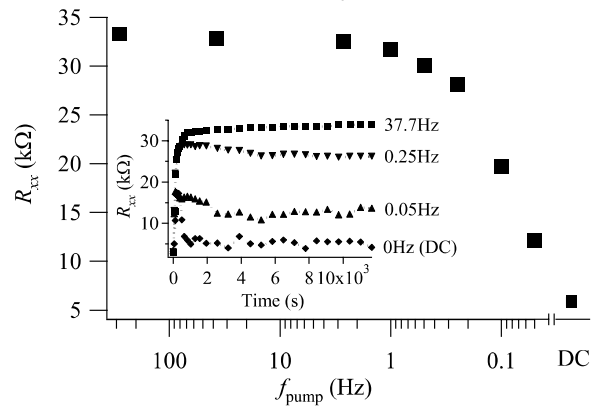


Fig.2. The pump current frequency f_{pump} dependence of RES.

References

- [1] S. Kraus, O.Stern, J. G. Lok, W. Dietsche, K. von Klitzing *et al.*, Phys. Rev. Lett. **89** (2002) 266801.
- [2] S. Tsuda, M. H. Nguyen, A. Fukuda, Y. Zheng, T. Arai and A. Sawada, 31st ICPS proceedings (2012).
- [3] S. Tsuda, M. H. Nguyen, D. Terasawa, A. Fukuda and A. Sawada, submitted to J. Phys. Soc. Jpn.

Novel mesophase in the region between Cholesteric and Perforated Lamellar -Nematic phases

Softmatter physics group, Jun Yoshioka

Abstract We experimentally analyzed the system where fluorinated amphiphiles are dispersed in the cholesteric solvent using the measurements of the layer compression, the translational diffusion, and the viscosity constants. In summary, we found a novel mesophase (Ch2) appears between the cholesteric and the perforated lamellar-nematic phases.

© 2013 Department of Physics, Kyoto University

Introduction

Recently, we found the perforated lamellar-nematic (PLN) phase appears in the system where the amphiphilic molecules (BI) having both a hydrocarbon and a fluorocarbon chain are dispersed in the thermotropic nematic solvent. In the PLN phase, the perforated bilayer structure is embedded in the nematic solvent. In this paper, by introducing the chirality into the nematic solvent, we realized the system where the BI molecules are dispersed in the cholesteric (Ch) liquid crystal, and found the novel mesophase (Ch2) appears between the Ch and the PLN phases. We also discussed the physical properties of the novel Ch2 phase using several experiments.

Results and Discussion

First, using the polarized microscopy, we made a concentration-temperature phase diagram of the mixture as shown in Fig.1. The Ch phase appears when the concentration of BI is low (0~30wt. %), while the PLN phase appears when the concentration of BI is high (35~50wt. %). In the sandwich cell where the helical axis is forced to be parallel to the glass substrates, we found the texture of the sample significantly changes dependent on the temperature in 28~35 wt. % BI mixture. Here, we speculated a novel mesophase appears in the region between the Ch and the PLN phase (hatched region), and call this new mesophase as the Ch2 phase.

Second, in order to confirm the existence of the Ch2 phase, we measured temperature dependence of the layer compression modulus as shown in Fig.2. The Ch phase has a pseudo-layer structure derived from its helix, so that it has a non-zero layer compression modulus along the helical axis. In the Ch phase, the layer compression modulus shows 10^3 – 10^4 N/m², which is the typical value in the conventional Ch phase. The modulus starts to increase just below the Ch-Ch2 transition temperature, and it attains to 10^6 N/m² in the Ch2 phase at 40°C. This result shows the Ch2 phase has a much stiffer layer structure.

Furthermore, we also detected the Ch-Ch2 transition by the translational diffusion constants and the viscosity modulus measurements. Thus, the Ch2 phase can be identified as a novel mesophase due to the frustration between the layer order of the aggregates of the BI molecules and the helical structure of the solvent.

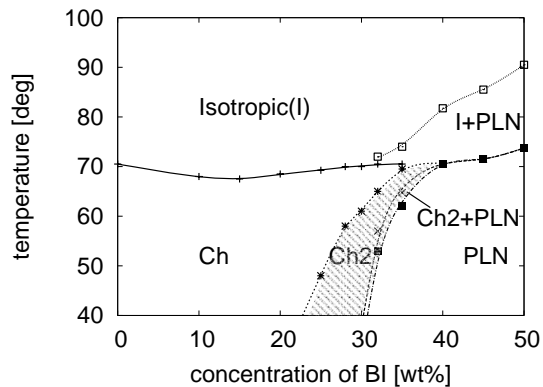


Fig. 1. Phase diagram

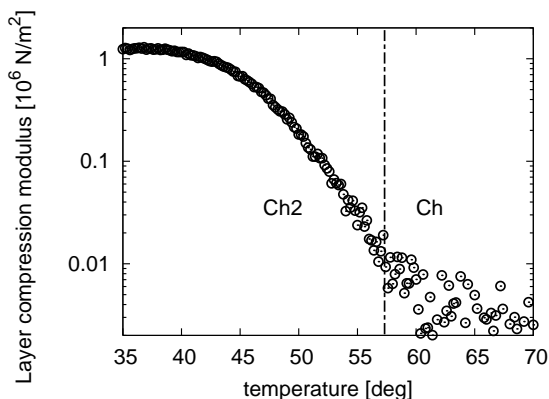


Fig. 2. Temperature dependence of layer compression modulus in 30wt. % BI mixture